DOI: 10.13009/EUCASS2017-412

Dusty Plasma Void Dynamics in Unmoving and Moving Flows

O.V. Kravchenko, O.A. Azarova**, and T.A. Lapushkina****
**Scientific and Technological Center of Unique Instrumentation of RAS*
Russia, Moscow, 117342, Butlerova str. 15
***Dorodnicyn Computing Centre, Federal Research Center*
"Computer Science and Control" of RAS
Russia, Moscow, 119333, Vavilova str. 40
****Ioffe Institute*
Russia, Saint Petersburg, 194021, Politekhnicheskaya str. 26

Abstract
Generation of steady structures with empty regions (voids) has been modelled numerically in unmoving and moving flows of dusty plasma. The simulations are based on the known model of Avinash, Bhattacharjee and Hu of formation of a void in a dusty plasma flow. The model has been reduced to the divergent form and two algorithms of first and second orders for calculations have been suggested. The Lax's scheme and the complex conservative difference scheme have been used for the first and second order for the hydrodynamic part of the model. Results on the dynamics of voids have been obtained at the stage of circular ring structure generation and at the final stage of a steady round void formation. Behaviour of the defining flow parameters has been obtained up to the steady dusty plasma flow mode. Description of the experimental installations for investigations of dusty plasma moving and unmoving flows and generation of structures in these flows has been presented.

1. Nomenclature

n_d, n_e	=	concentrations of dust and electrons components
v_d, v_i	=	velocities of dust and ions components
E	=	electric field currency
F_d	=	ion-drag force
D_0	=	diffusion coefficient
t, x, y	=	time and spatial variables
a, b	=	fit parameters of ion-drag force approximation
μ	=	coefficient of ions mobility
α_0	=	friction coefficient
τ_d, τ_i	=	coefficients of normalized temperature for dust and ion species
n_i	=	amount of the grid points in the x-direction

Index "$_0$" refers to the initial parameters
DC Direct current

2. Introduction

A number of the investigations of the dynamics of dusty plasma were published in recent years [1, 2]. At the same time, it is not so much studies in which the numerical simulations of the structure generation in dusty plasma are performed. The first dusty plasma structure containing empty domains (voids) was discovered in the course of the experiments on the board of the International Space Station [2]. Also, in the laboratory conditions the voids have been found later [3-5]. Evolution of the dynamics of a single symmetric void from equilibrium was described by electro-hydrodynamic model [6, 7] taking into account the effect of an ion attraction force as a nonlinear function of the speed of ions. The algorithm for simulations of appearance of

DOI: 10.13009/EUCASS2017-412

dusty plasma void using the model [7] has been presented in [8] for the case of cylindrical geometry of the electrical field. Generation of a single symmetric void and concentric symmetrical voids in unmoving flows of low-temperature dusty plasma has been obtained in [9].

A study of generation of voids in moving flows together with the further research of the voids in unmoving media is a purpose of this paper. The simulations are based on the model [7] of formation of a void in the dusty plasma flow. The Lax's scheme and the complex conservative difference scheme [10] have been used in the first and second order approaches for the hydrodynamic part of the model.

3. Methodology

3.1 Description of the using physical model

Simulations are based on the difference schemes of the first and second order of approximation of the model [7]. Here the model is considered in dimensionless form, believing that the normalizing parameters from [7] have been applied:

$$\frac{\partial v_d}{\partial t}+v_d\frac{\partial v_d}{\partial x}=F_d-E-\alpha_0 v_d-\frac{\tau_d}{n_d}\frac{\partial n_d}{\partial x}, \tag{1}$$

$$\frac{\partial n_d}{\partial t}=-\frac{\partial(n_d v_d)}{\partial x}+D_0\frac{\partial^2 n_d}{\partial x^2}, \tag{2}$$

$$\frac{dn_e}{dx}=-\frac{n_e E}{\tau_i}, \tag{3}$$

$$\frac{dE}{dx}=1-n_e-n_d, \tag{4}$$

$$F_d=\frac{aE}{b+|v_i|^3},\quad v_i=\mu E. \tag{5}$$

Here n_d, n_e are concentrations of dust and electrons components, v_d, v_i are velocities of dust and ions components, E is electric field currency, F_d is ion-drag force, D_0 is diffusion coefficient. In fact the governing equations in this model contain dust momentum (1) and dust continuity equations (2), balance equation on electrons neglecting the electron inertia (3). Poisson law which completes the nonlinear system of equations, and the expression for ion–drag force are presented in (4, 5). It should be noticed that ion–drag force (5) is a force which acts on dust particles from ions and is approximated by nonlinear function with fit positive constants a, b. Equations (1) and (2) constitute the hydrodynamic part of the model and the equations (3)-(5) are the electrostatic part of it.

One of the major features of the model [7] is that ion–drag force F_d depends on the ion velocity v_i and it decreases with the increase of the velocity as a cubic function of v_i. Also, this model is a self–consistent system of partial differential equations in which the dynamics of the charged component of medium effects on electrical field distribution E and vise versa electrical field distribution effects on a motion of charged particles. One could realize that densities of dust particles, electrons and ions are the unknown functions as well as electrical field distribution function E. Velocity of ions v_i is linearly proportional to electrical field distribution E with coefficient of proportionality μ.

3.2 Description of the numerical models with the first and second order of difference schemes for hydrodynamic part of the model

A general algorithm of the numerical simulation for the first order model from [7] (1)–(4) which was introduced recently [8] is as follows:

DOI: 10.13009/EUCASS2017-412

- Computation of the initial–value problem of (1), (2) with Neumann boundary condition by explicit conservative scheme (the Lax's scheme in the first order case) on current time step of integration t^n, so n_d, v_d are known functions on the current time step.
- Computation of the initial–value problem of (3),(4) by explicit solver of Cauchy problem on the same time step of integration t^{n+1}, so n_e, E are known functions on the current time step t^n also. Here the method of Runge-Kutta of the forth approximation degree is used.
- Recomputation of (1), (2) with Neumann boundary condition on the next time step of integration t^{n+1} with respect to previous items, so n_d, v_d are known functions on the next time step t^{n+1}.

For the first order calculations of the hydrodynamic part of the model the Lax's scheme is used (with D_0=0) for the divergent form of the equations (1), (2):

$$\frac{\partial \mathbf{u}}{\partial t}+\frac{\partial \mathbf{F}}{\partial x}=\mathbf{f}, \tag{6}$$

where

$$\mathbf{u}=\begin{pmatrix} n_d \\ v_d \end{pmatrix}, \mathbf{F}=\begin{pmatrix} n_d v_d \\ 0.5 v_d^2+\tau_d \ln n_d \end{pmatrix}, \mathbf{f}=\begin{pmatrix} D_0 \dfrac{\partial^2 n_d}{\partial x^2} \\ F_d-E-\alpha_0 v_d \end{pmatrix}.$$

The second order scheme for the algorithm [8, 9] was obtained (without recomputation) using the approach of [10] for increasing the difference scheme order. By this way the systems of divergent equations (6) are used for unknown functions together with the system for their space derivatives:

$$\frac{\partial \mathbf{u_x}}{\partial t}+\frac{\partial \mathbf{F_x}}{\partial x}=\mathbf{0}, \tag{7}$$

where

$$\mathbf{u_x}=\begin{pmatrix} n_{dx} \\ v_{dx} \end{pmatrix}, \mathbf{F_x}=\begin{pmatrix} (n_d v_d-D_0 n_{d\,x})_x \\ (0.5 v_d^2+\tau_d \ln n_d)_x+E-F_d+\alpha_0 v_d \end{pmatrix}.$$

In the systems of the derivatives (7) the space derivatives from the right parts are included into the flux functions. It provides the absence of the numerical (parasite) sources and runoffs. Equations (3), (4) are approximated with the second approximation order using the central form for the space derivatives and the method of Runge-Kutta of the fourth order of approximation is used, too.

In the numerical simulations the next restrictions were imposed: if n_d>1 then n_d was applied by 1 and v_d was applied by v_{d0}.

4. Numerical simulations

Numerical experiments on generation of voids in the flows of dusty particles have been conducted for zero and nonzero initial velocity v_{d0} of a dusty component. Parameters of the simulations are collected in Tab. 1.

4.1 Comparison of the simulations using the first and the second order models

Comparison of the simulations using the difference schemes of the first and second approximation order is presented in Fig. 1. It can be seen that the obtained dynamics are quite the same (Fig. 1a). It should be noted that the restrictions on v_d is introduced for "cutting" the high frequency numerical oscillations in the dynamics of v_d (when n_d becomes more than 1). These oscillations are seen in the profile of n_d calculated with the use of the second order scheme (Fig. 1b, *red curve*). Introduction into the scheme the term with the diffusion of concentration of the dusty component (which plays the role of "viscosity" in (2)) allowed smoothing these oscillations (Fig. 1b, *black curve*, D_0=0.1). Note that the diffusion term is introduced into the difference approximations via the flux function in (7).

DOI: 10.13009/EUCASS2017-412

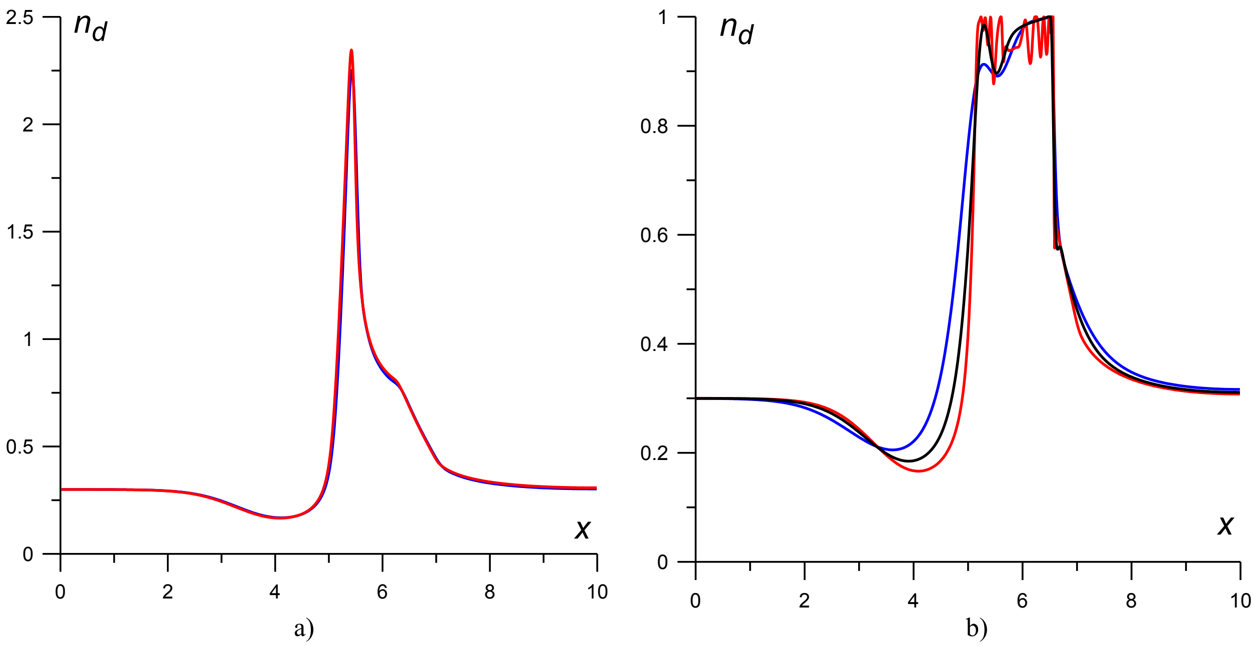

Figure 1: Comparison of dynamics of concentration of dusty component n_d during the void formation calculated with the use of first (*blue curve,* D_0=0) and second (*red curve,* D_0=0) order schemes for the hydrodynamic part of the model, n_{d0}=0.3, v_{d0}=0, 1: a) beginning stage (without the restrictions on n_d and v_d); b) subsequent stage (with the restrictions on n_d and v_d), *black curve* - D_0=0.1

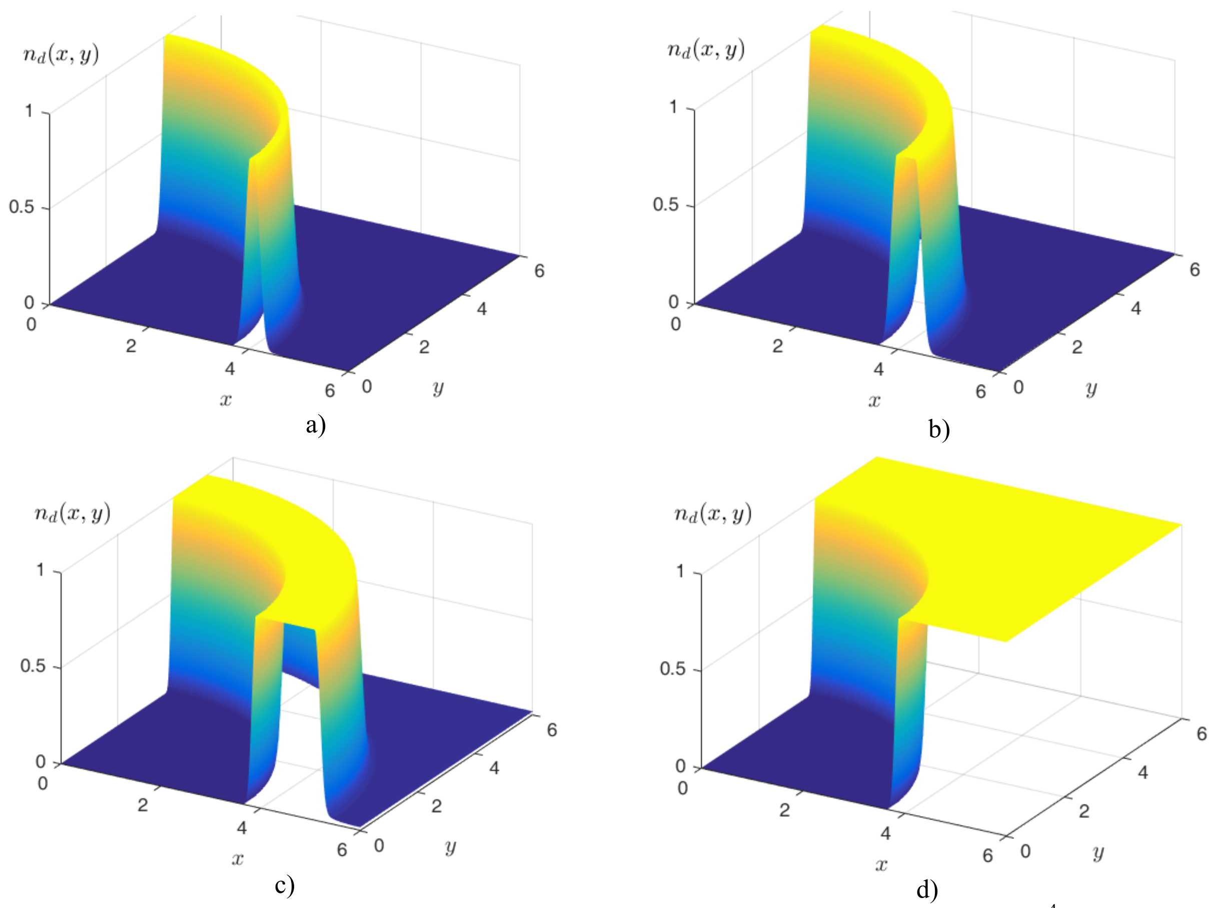

Figure 2: Dynamics of concentration of dusty component n_d during the void formation, E_0= $4\cdot10^{-4}$ (first order scheme): a) - non-dimensional time t=70 (unsteady ring structure); b) - t=100; c) - t=140; d) - t=200 (steady void)

DOI: 10.13009/EUCASS2017-412

4.2 Modeling of dynamics of generation of void in unmoving flows

Dynamics of generation of a void in the unmoving flow (v_{d0}=0) of dusty particles with the use of the first order algorithm for the hydrodynamic part is shown in Fig. 2. Two-dimensional figures for n_d obtained by the rotation technique are presented. The mechanism of generation of voids is connected with the superposition of the electrical field and the ion attraction force action. Void grows in time from the constant parameters and becomes saturated at time moment t=200 (Fig. 2d). The transitional states are presented in Figs. 2a-2c at time moments t=70, 100, 140, respectively. It can be seen that at the first stage the ring structure is forming with a void generated in a centre of it. Then the right boundary of this structure moves right and leaves the calculation area keeping the constant parameters behind it.

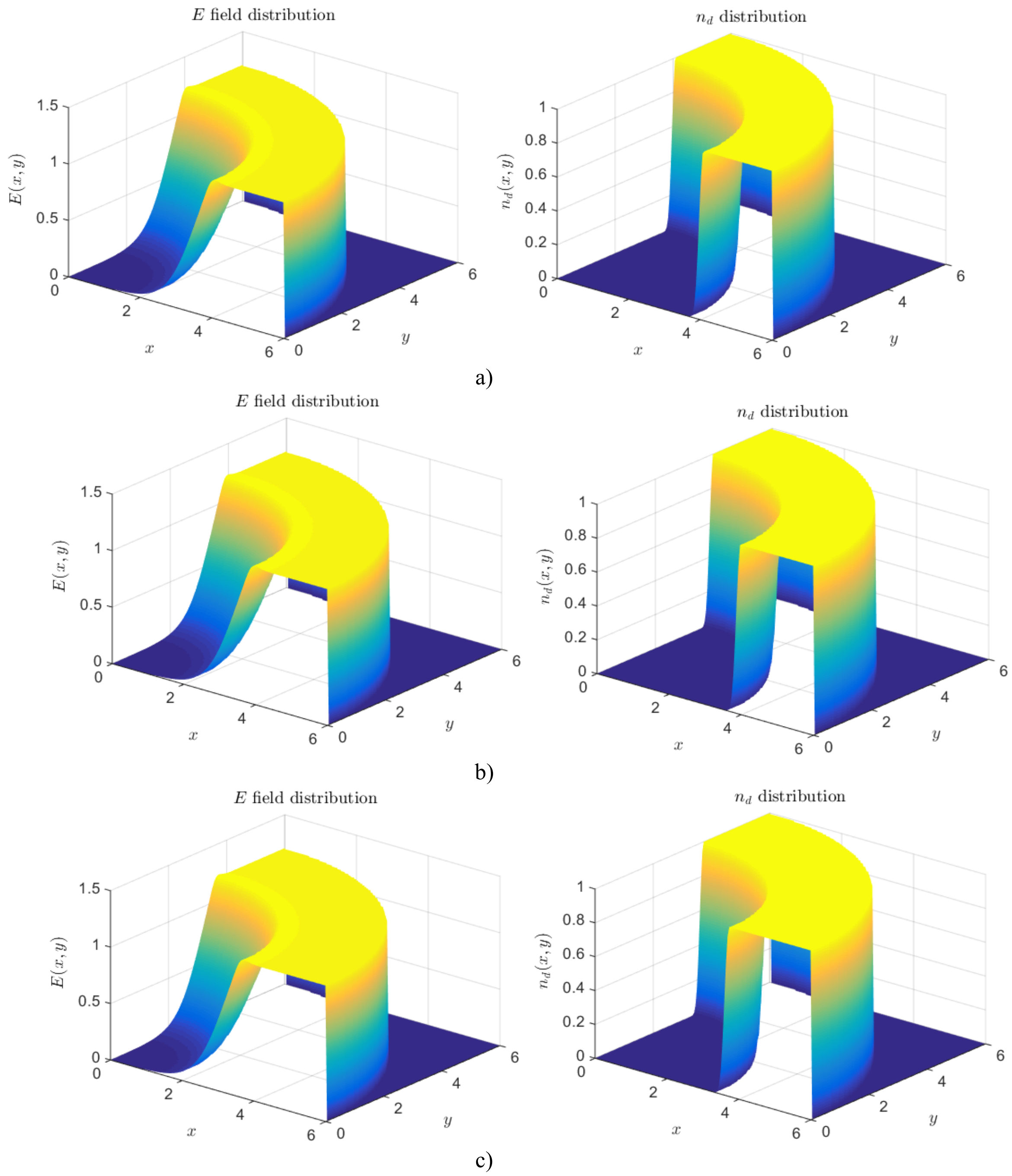

Figure 3: Dependence of n_d distributions on initial value of the electric field E_0, t=200 (first order scheme): a) E_0= $4 \cdot 10^{-6}$; b) E_0= $4 \cdot 10^{-5}$; c) E_0= $4 \cdot 10^{-4}$

DOI: 10.13009/EUCASS2017-412

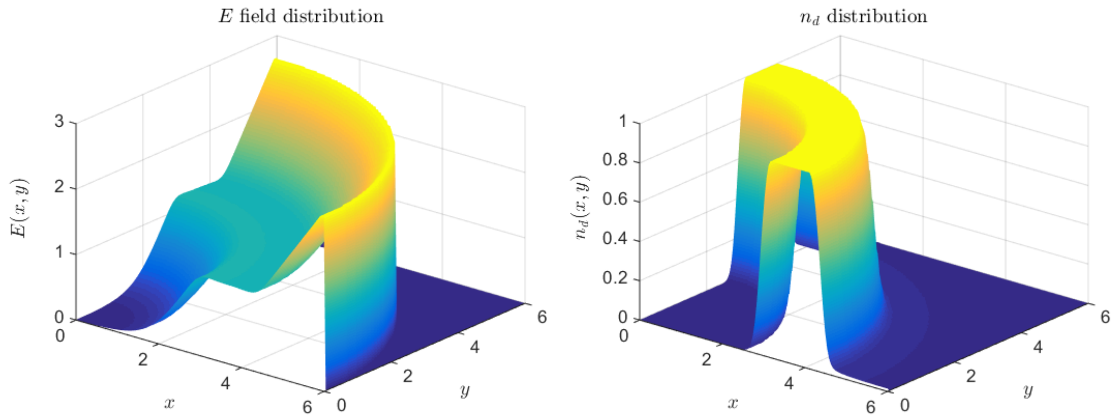

d)

Figure 3 (continuation): Dependence of n_d distributions on initial value of the electric field E_0, t=200 (first order scheme): d) E_0= $4\cdot10^{-3}$

Distribution of n_d for different initial distributions of the electric field E is presented in Fig. 3. Here the beginning stage with generation of the ring structure of dusty particles is presented. One could find that the size of a void region decreases while the initial value E_0 increases from 10^{-6} (Fig. 3a) to 10^{-3} (Fig. 3d). For E_0=10^{-6} the void's radius is close to 4 (Fig. 3a) while it is about 2.2 for E_0=10^{-3} (Fig. 3d). From the other hand, it could be found that there is a semi-saturated state of the void's formation inside the generated ring structure of dusty particles.

Table 1: Simulation parameters of the numerical experiment

Parameters	Values
τ_i	0.125
τ_d	0.001
a	7.5
b	1.6
α_0	2
μ	1.5
n_{e0}	0.999

Dynamics of generation of a void with the use of the second order difference scheme for the hydrodynamic part of the model [7] is shown in Fig. 4 (here D_0=0.1, b=2). The blue curve presents the profile of n_d at thebeginning stage of the unsteady concentric ring structure formation and the green and red curves correspond to the stage of the steady void formation in the central area (Fig. 4a). Figure 4b demonstrates the profiles of all the defining parameters for the steady flow containing the formed void. Two-dimensional figures for n_d obtained by the rotation technique are presented in Figs. 4c, 4d. It can be seen that the presence of diffusion of the concentration increases the values of n_d at the void's center (Fig. 4c) but by changing the constant b in the expression of the ion-drag force F_d (5) the value of residual dusty component concentration can be decreased into the void (Fig. 4d, b=0.4), the decrease of n_{d0} being obtained to provide some icrease of the void's radius.

4.3 Modeling of dynamics of generation of void in moving flows

Dynamics of generation of a void in the moving flow (v_{d0}=0.1) of dusty particles with the use of the first order scheme for the hydrodynamic part of the model [7] is presented in Fig. 5. Here all the defining parameters are shown at the stage of establishing the steady flow mode (Figs. 5a, 5b). The void which was formed at this quasi-steady mode is shown in Fig. 5c using the rotation technique. Dynamics of the void boundary (*curve 1*) and the value of v_d for $x(n_i)$ (*curve 2*) are presented in Fig. 6. It can be seen that the velocity of the dusty

DOI: 10.13009/EUCASS2017-412

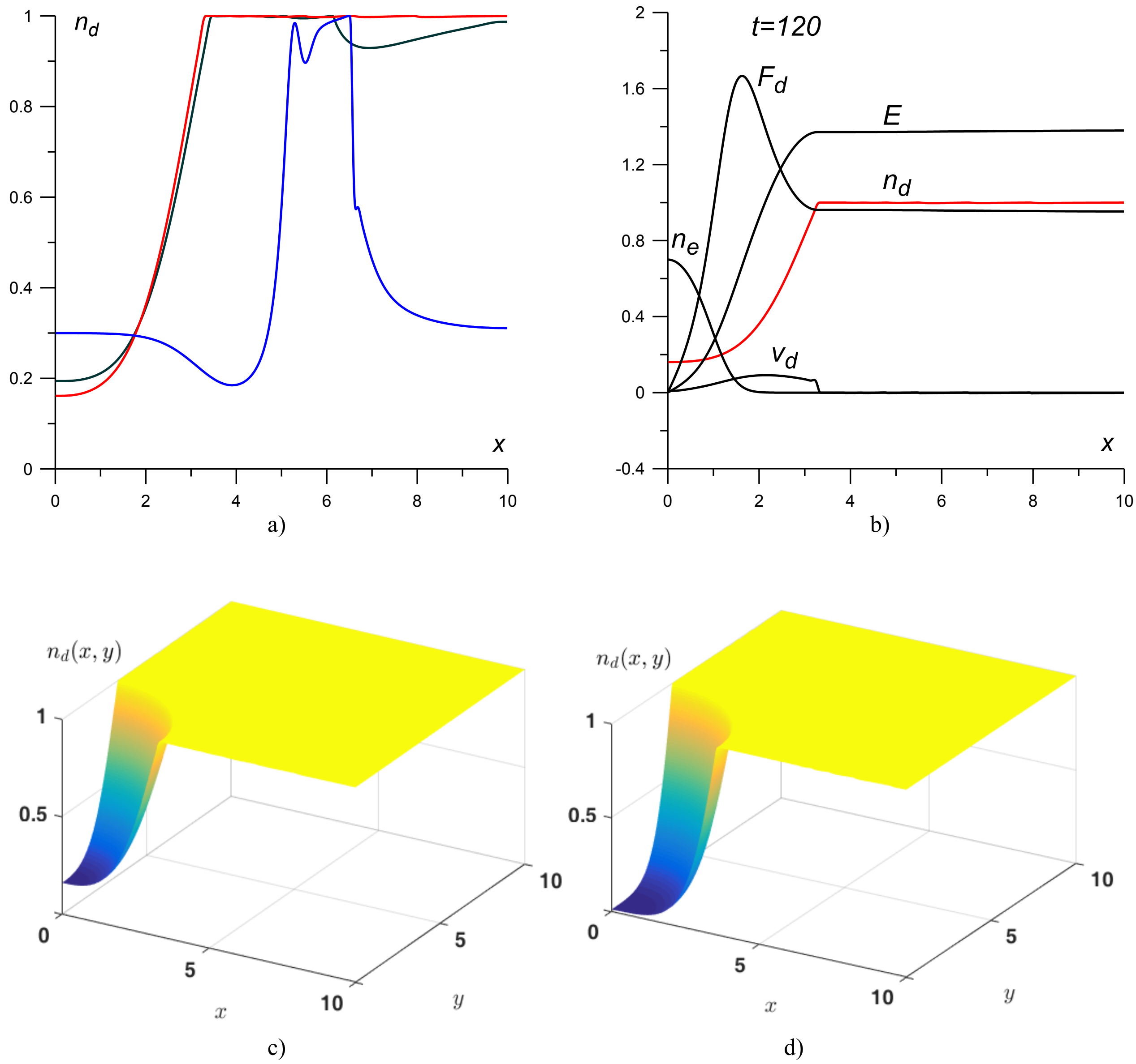

Figure 4: Simulations with the use of second order scheme, n_{d0}=0.3, b=2 (a) – (c), n_{d0}=0.2, b=0.4 (d), v_{d0}=0, E_0= $4\cdot10^{-5}$, n_i=2000, D_0=0.1: a) - dynamics of concentration of dusty component n_d during the a void formation: t=20 (*blue*), t=60 (*green*), t=120 (*red*); b) - profiles of the defining flow parameters on the stage when the steady void is formed, t=120; c), d) - steady voids obtained (n_d), t=120

component (*curve 2*) performs the oscillations of small amplitude which is connected with the applied restriction on v_d. Nevertheless the void boundary (*curve 1*) is shown to be a converging curve. It has to be noted that it could be interesting to provide such type of the restrictions which would cause the oscillations of the void's boundary.

Dynamics of generation of a void in the case of v_{d0}=0.3 is presented in Fig. 7. Here all the defining parameters at the stage of establishing the steady flow mode are shown (Figs. 7a) and the void obtained at this quasi-steady mode is shown in Fig. 7b using the rotation technique. It is seen the non-monotonic behavior in the distribution of concentration of dusty particles n_d which may be connected with a simple waves effect in periphery area of the void.

DOI: 10.13009/EUCASS2017-412

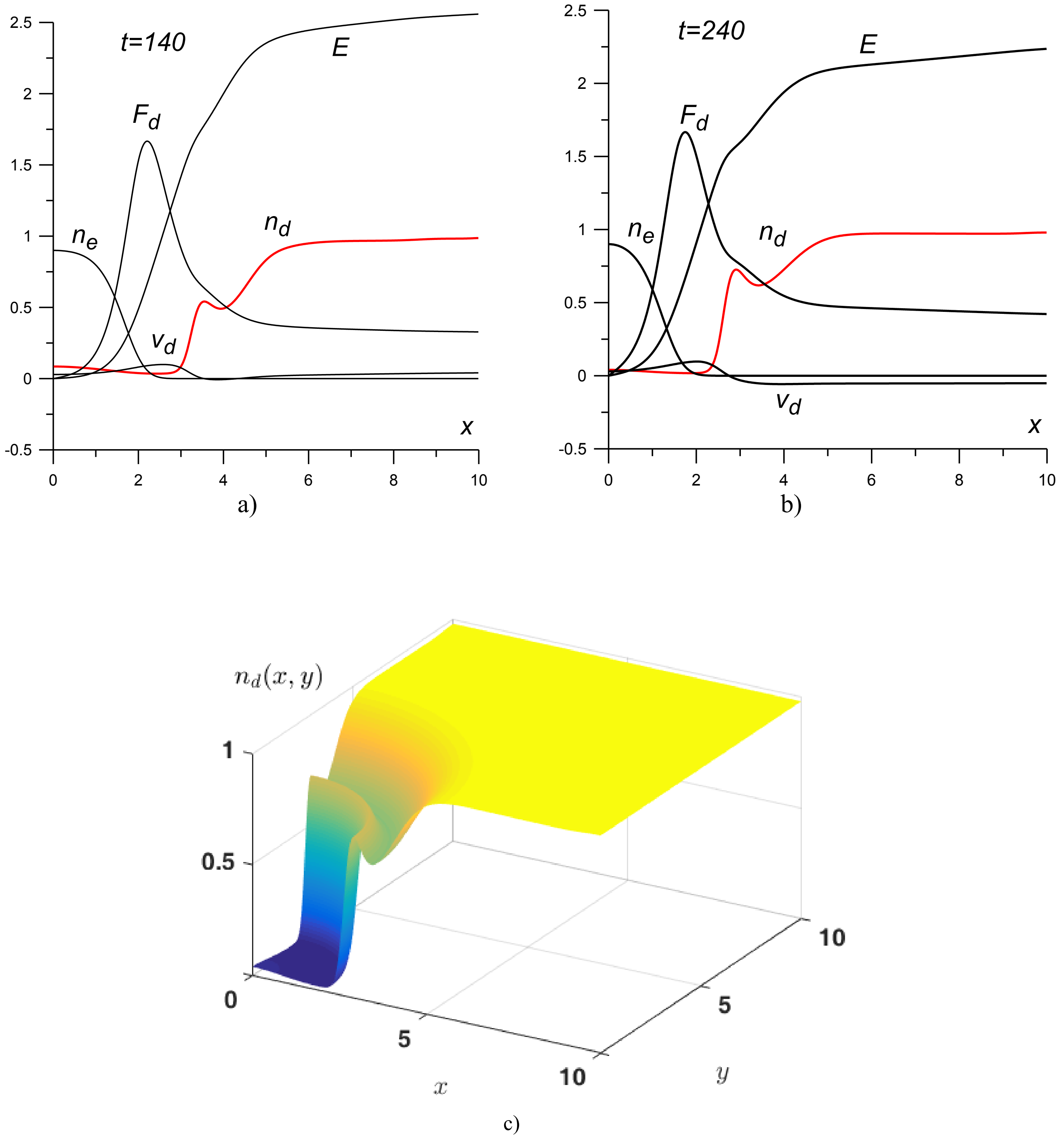

Figure 5: Profiles of the defining flow parameters on the stage establishinh the steady void formation, first order scheme, n_{d0}=0.1, v_{d0}=0.1, E_0= $4\cdot10^{-5}$, n_i=2000, b=2: a) - t=140 ; b) - t=240; c) – distribution of n_d in quasi-steady flow mode, t=240

DOI: 10.13009/EUCASS2017-412

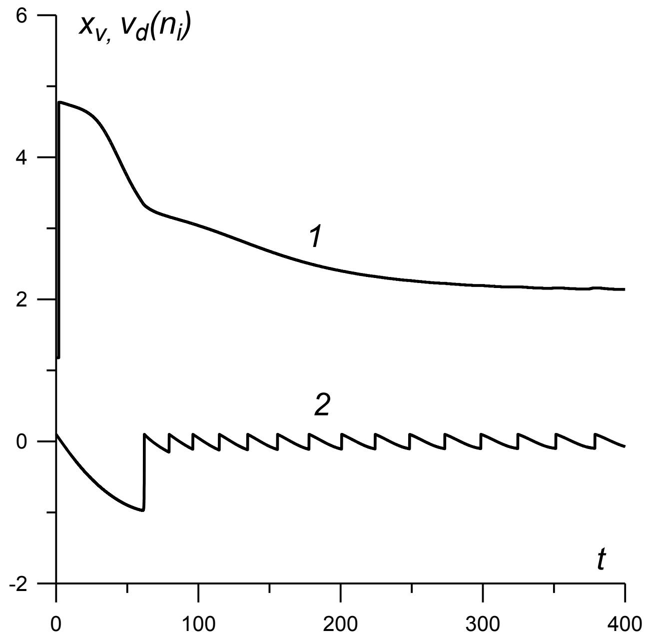

Figure 6: Dynamics of the void's boundary (*curve 1*) and the value of v_d in $x(n_i)$ (*curve 2*), first order scheme, n_{d0}=0.1, v_{d0}=0.1, E_0= $4\cdot10^{-5}$, n_i=2000

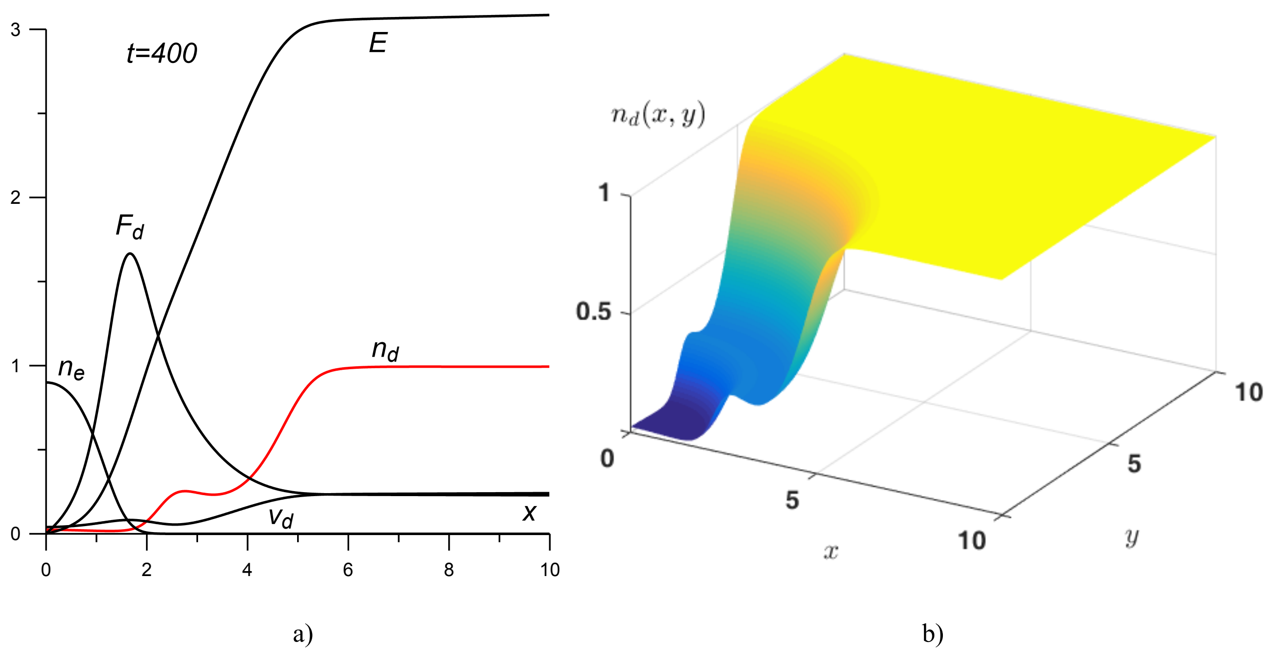

a) b)

Figure 7: a) - profiles of the defining flow parameters at the stage of the steady void formation, first order scheme, n_{d0}=0.1, v_{d0}=0.3, E_0= $4\cdot10^{-5}$, n_i=2000, t=400; c) – quasi-steady void obtained (n_d), t=400

DOI: 10.13009/EUCASS2017-412

5. Experimental installations (principal schemes and description)

Here two experimental installations are described for planned investigations of dynamics of dusty plasma flows and formation of dusty plasma structures including generation of voids in unmoving and moving flows.

5.1 Experimental installation for investigation of dusty plasma flows in unmoving media

For investigation of dusty plasma including generation of voids in unmoving media the next experimental set up is planned to be developed on a base of the existing one.
The installation for investigation of plasma dynamic in unmoving media (Fig. 8) consists from the working chamber with diameter 300 mm and height 400 mm. Two conical electrodes are disposed vertically along the camber axis at the distance 100 mm from each other. DC voltage which applied to the electrodes produces a stationary glow gas discharge at the varying pressure in changeable gases including a gas with dust particles. It allows producing dusty plasma in unmoving media. In the discharge region the gas temperature is about 1500 K, electron temperature is about 12000 K and ionization degree is about 10^{-6}. The electro-discharge shock tube with diameter 40 mm and length 700 mm is disposed at the lateral wall of the chamber. It allows producing shock wave with velocity about 1.3 km/s, at Mach number 3.8. The installation has the electrical probe, piezo probe for pressure measurement, the optical Schliren system and devices for optical and spectrographic measurements.

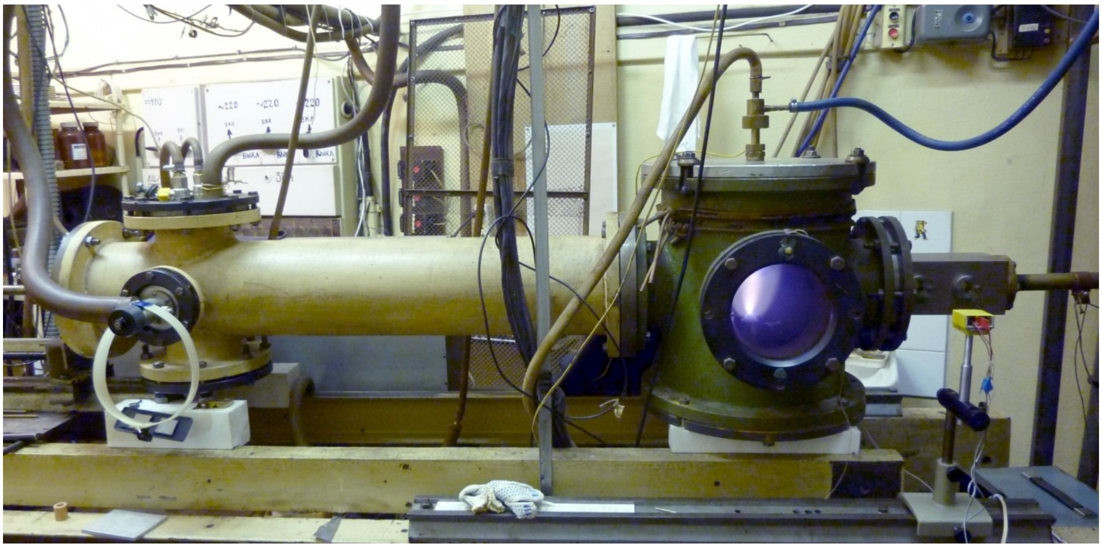

Figure 8: The installation for investigation of dusty plasma dynamics in unmoving media (photo)

5.2 Experimental installation for investigation of dusty plasma moving flows

For investigation of dynamics of dusty plasma including generation of voids in moving flows the next experimental set up is planned to be developed on a base of the existing one.
The shock tube is collected from the stainless steel welded sections of the rectangular cross section 50x150 mm^2, 1m length (Fig. 9). The plates are polished and the sections are welded, which allows getting the flow with the small perturbations of the gasdynamic parameters behind a shock wave front. The general length of shock tube is 10 m. As the shock tube consists of some sections the relative sizes of the high pressure chamber and low pressure channel can be changed depending on required work regime. For creation of shock waves with Mach numbers M > 7, the gas in the high pressure chamber can be additionally heated up to 200 – 400 C.
The rectangular cross section of the tube allows studying the stationary homogeneous non-divergent flows of the different gas composition in the wide diapason of Mach numbers including the flows with additional injection of micro particles. So it is possible to create the homogeneous ionized gas discharge zones in the flow

DOI: 10.13009/EUCASS2017-412

with micro particles and to form a flow of dusty plasma. In future it will allow investigating the appearance and changing new gas dynamic structures and generation of voids in moving dusty plasma flows.

Figure 9: The installation on the base of the rectangular cross section shock tube for study of moving dusty flows (photo)

6. Summary

- Known model of Avinash, Bhattacharjee, and Hu of formation of a void in the dusty plasma flow has been rewritten in the divergent form and the numerical algorithms of the first and second approximation order for the hydrodynamic part of the model have been developed.
- Numerical simulations with the use of the obtained numerical models were conducted and the results on the void generation and dynamics have been obtained in unmoving and moving flows of dusty plasma.
- Dependence of the concentration of dusty particles on the initial value of the electric field was obtained. It has been shown that the size of a void region decreases when the initial value of the electric field increases.
- Results on behavior of the profiles of all the defining parameters at the stage of the concentric ring structure formation and at the stage of the formed void existence in the steady flow mode have been obtained.
- Description of the experimental installations for future experimental investigations of dusty plasma moving and unmoving flows and generation of structures in these flows (including formation of the voids) has been presented.

References

[1] Molotkov, V., H. Thomas, A. Lipaev, V. Naumkin, A. Ivlev, and S. Khrapak, 2015. Complex (dusty) plasma research under microgravity conditions: PK-3 Plus Laboratory on the International Space Station. *International Journal of Microgravity Science and Application.* 35(3):1–8.

[2] Fortov, V.E., G.E. Morgill. 2009. Complex and dusty plasmas: from laboratory to Space. CRC Press: 401.

[3] Feng, H., Y. Mao-Fu, W. Long, and J. Nan. 2004. Voids in experimental dusty plasma. *Chin. Phys. Lett.* 21(1):121–124.

DOI: 10.13009/EUCASS2017-412

[4] Sarkar, S., M. Mondal, M. Bose, and S. Mukherjee. 2015. Observation of external control and formation of a void in cogenerated dusty plasma. *Plasma Sources Sci. Technol.* 24(3):1–7.
[5] Feng, H., Y. Maofu, and W. Long. 2006. Pattern phenomena in an RF discharge dusty plasma system. *Science in China Series G: Physics, Mechanics & Astronomy*. 49(5):588–596.
[6] Ng, C.S., A. Bhattacharjee, S. Hu. Z.W. Ma, and K. Avinash. 2007. Generalizations of a nonlinear fluid model for void formation in dusty plasmas. *Plasma Phys. Control. Fusion*. 49:1583–1597.
[7] Avinash, K., A. Bhattacharjee, and S. Hu. 2003. Nonlinear theory of void formation in colloidal plasmas. *Phys. Rev. Lett.* 90(7):1–4.
[8] Kravchenko, O.V., and V.I. Pustovoit. 2016. Numerical simulation of dynamics of concentric dusty–plasma structures. In: *15th International Workshop on Magneto–Plasma Aerodynamics.* 1–8.
[9] Kravchenko, O.V. Simulation of spatially localized dusty plasma structures in complex plasma. 2016. *Nanostructures. Mathematical physics and modeling*. 15(2):51–61 (in Russian).
[10] Azarova, O.A. Complex conservative difference schemes for computing supersonic flows past simple aerodynamic forms. 2015. *J. Comp. Math. Math. Phys*. 55(12):2067–2092.